# NEUTRON DOSIMETRY AND SPECTROSCOPY

# USING BUBBLE DETECTORS

# AND AN ANTHROPOMORPHIC PHANTOM

HUGUES W. BONIN, GUY DESNOYERS AND THOMAS COUSINS[1]

DEPARTMENT OF CHEMISTRY AND CHEMICAL ENGINEERING

ROYAL MILITARY COLLEGE OF CANADA

KINGSTON, ONTARIO, CANADA K7K 5L0

1. Radiation Effects Section
   Electronics Division
   Defence Research Establishment Ottawa
   Ottawa, Ontario, Canada K1A 0Z4
   Tel.: 613-998-2312

Presented at the 13th Annual Conference of the Canadian Nuclear Society, St. John, New Brunswick, 7-10 June 1992.

# NEUTRON DOSIMETRY AND SPECTROMETRY USING BUBBLE DETECTORS AND AN ANTHROPOMORPHIC PHANTOM

HUGUES W. BONIN[1*], GUY DESNOYERS[1], AND THOMAS COUSINS[2]

1. Dept. Chemistry and Chemical Engineering
Royal Military College of Canada
Kingston, Ontario, Canada K7K 5L0
613-541-6613; FAX: 613-542-9489

2. Radiation Effects Section, Electronica Division
Defence Research Establishment Ottawa
Ottawa, Ontario, Canada K1A 0Z4
613-998-2312

*: Author to whom correspondence should be addressed.

## ABSTRACT

Neutron kermas and energy spectra at various positions in and on an anthropomorphic phantom irradiated with a Californium-252 source were experimentally determined using superheated drop or bubble detectors. The results obtained permit determination of the optimal wearing position of one (or more) dosimeters to relate their readings to free-field kerma.

Overall conclusions of the performance of the BD-100R dosimeter and BDS spectrometer sets were also derived, with the BD-100R proving superior in terms of accuracy and reproducibility.

## Introduction

In 1987, the Canadian Navy was directed to proceed with a proposal for the eventual acquisition of nuclear-powered submarines. The dosimetry involved on-board submarines is unique in that the contribution to the total dose from neutrons is much larger than for land-based reactors - owing to the biological shielding being limited by space and weight considerations. New radiological results from low dose experiments suggest a greater biological risk from neutron radiation than previously thought (1). In this context, it was decided to examine experimentally the neutron dose distribution throughout the human body.

To accomplish this, an anthropomorphic phantom was outfitted with bubble dosimeters and spectrometers and irradiated at a distance of 170 cm from a Californium-252 source. The results shed light on dosimeter performance, optimum dosimeter wearing positions and neutron transport through the body.

## The Anthropomorphic Phantom

The anthropomorphic phantom used here was a Humanoid RT-200 (2) embracing a human skeleton encased in tissue equivalent plastics - one for the lungs and the other for the bulk of the body. The Defence Research Establishment Ottawa (DREO) has performed neutron activation and chemical analyses on these plastics, and the results of these compared to the International Commission on Radiation Units and Measurements reference man composition (3,4) as shown in Table I. Note that for the body plastic, the all-important (for neutron scattering) hydrogen content is relatively high at 9.6%. Therefore the anthropomorphic phantom may be considered appropriate for neutron dosimetry and spectroscopy experiments.

Table I. RT-200 Phantom Composition (Weight Percent) (Ref. 2)

| ELEMENT VALUES | SOFT TISSUE | ICRP VALUES | LUNG TISSUE | ICRP |
|---|---|---|---|---|
| Hydrogen | 9.6 | 10.0 | 7.1 | 9.9 |
| Carbon | 65.4 | 18.0 | 60.6 | 10.0 |
| Nitrogen | 4.5 | 3.0 | 6.1 | 2.8 |
| Oxygen | 20 | 65.0 | 26 | 74.0 |
| Sodium | 0.000864 | --- | 0.000017 | --- |
| Aluminum | 0.000010 | --- | 0.000015 | --- |
| Chlorine | 0.000135 | --- | 0.001076 | --- |
| Manganese | ≈0 | --- | - | --- |
| Bromine | - | --- | 0.000011 | --- |
| Density ($g-cm^{-3}$) | 1.026 | | 0.390 | |

## The Bubble Detectors

The bubble detector, as originally developed by Ing (5), (6), consists of superheated droplets of a detector liquid dispersed in an elastic polymer gel. Neutron interactions in the vicinity of these droplets deposit enough energy locally to allow bubble nucleation, and the droplets expand until they reach a fixed diameter determined by a number of factors including pressure exerted by the gel. Simply by counting visually the number of bubbles and dividing by a calibration factor, dose equivalent or fluence information is obtained.

The detector employed here were the BD-100R (7) for dosimetry and the BDS spectrometer set (8) for spectrometry. Figures (1) and (2) give the measured energy responses for these detectors, as determined at the DREO Van de Graaf particle accelerator.

The BD-100R has been used extensively by DREO (2), (3), (8) and represents mature technology. Its efficacy as a dosimeter for the fission neutron free field is shown by the following results (Fig. 3) obtained from the measurement of the Mid-Line-Free-in-Air Kerma (MLFIAK) with the Californium-252 source.

The MLFIAK irradiation runs were performed frequently to determine the Free-in-Air Kerma and to establish a baseline to verify consistency of the results as the measurements proceeded with time. Twelve detectors were irradiated at each MLFIAK run and the detector responses were averaged and reported as kerma rates. The response for the 12 BD-100R detectors for the 10 different MLFIAK irradiation runs were summed up and averaged, giving a kerma rate of 0.58 mrad/hr.

The MLFIAK thus measured is the sum of the theoretical kerma rate and a scatter contribution which was determined experimentally with the use of a scatter bar. This theoretical kerma rate, simply the Watt spectrum for the neutron source, could be compared with the difference of the MLFIAK measured with and without the scatter bar. The comparison agreed well within error bars.

The BDS Spectrometry set, as can be seen from Figure (2), has approximate energy thresholds at 10 keV, 100 keV, 600 keV, 1.5 MeV, 2.5 MeV and 10 MeV. To obtain crude spectral information from the set, a simple spectral stripping algorithm was used here. Using the usual convention that the lowest number assigned to an energy group designates the fastest neutrons, then the observed number of bubbles in any spectrometer detector ($R_i$) corresponding to the number of neutrons having energies greater than its threshold energy ($E_i$) can be obtained from the following lower triangular matrix equation:

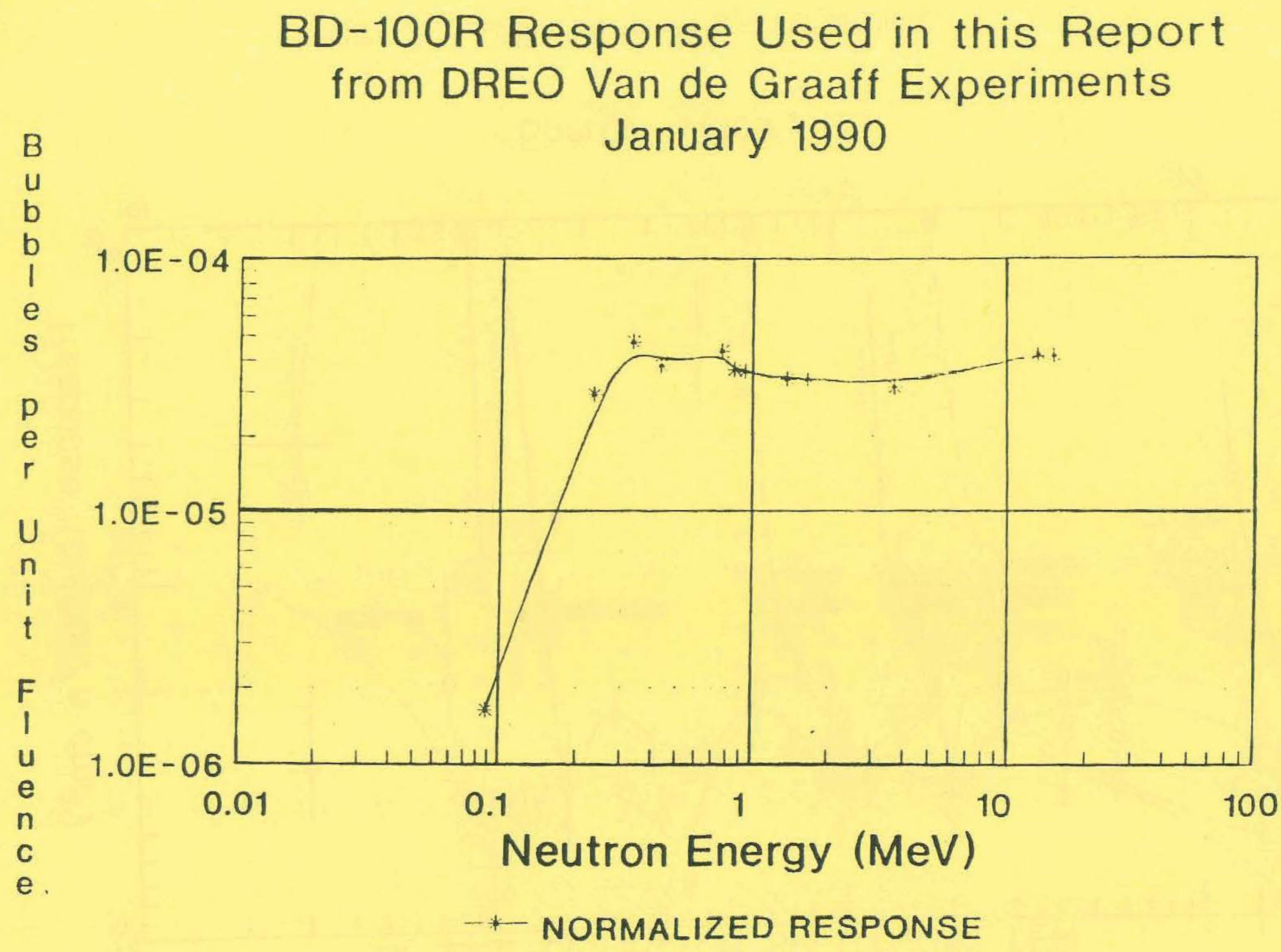


Figure 1 Bubble Detector Response.

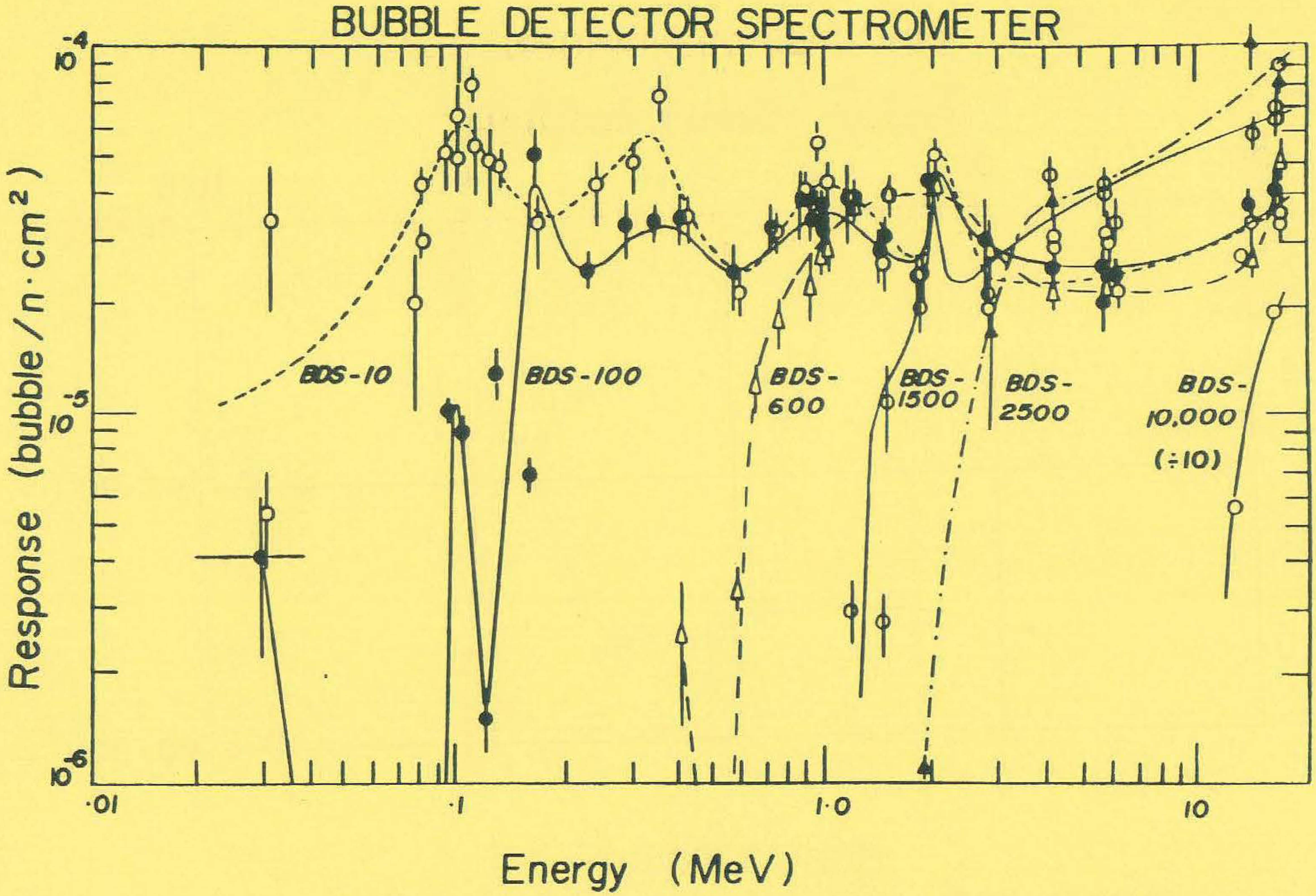


FIGURE 2 BDS FLUENCE/ENERGY RESPONSE.

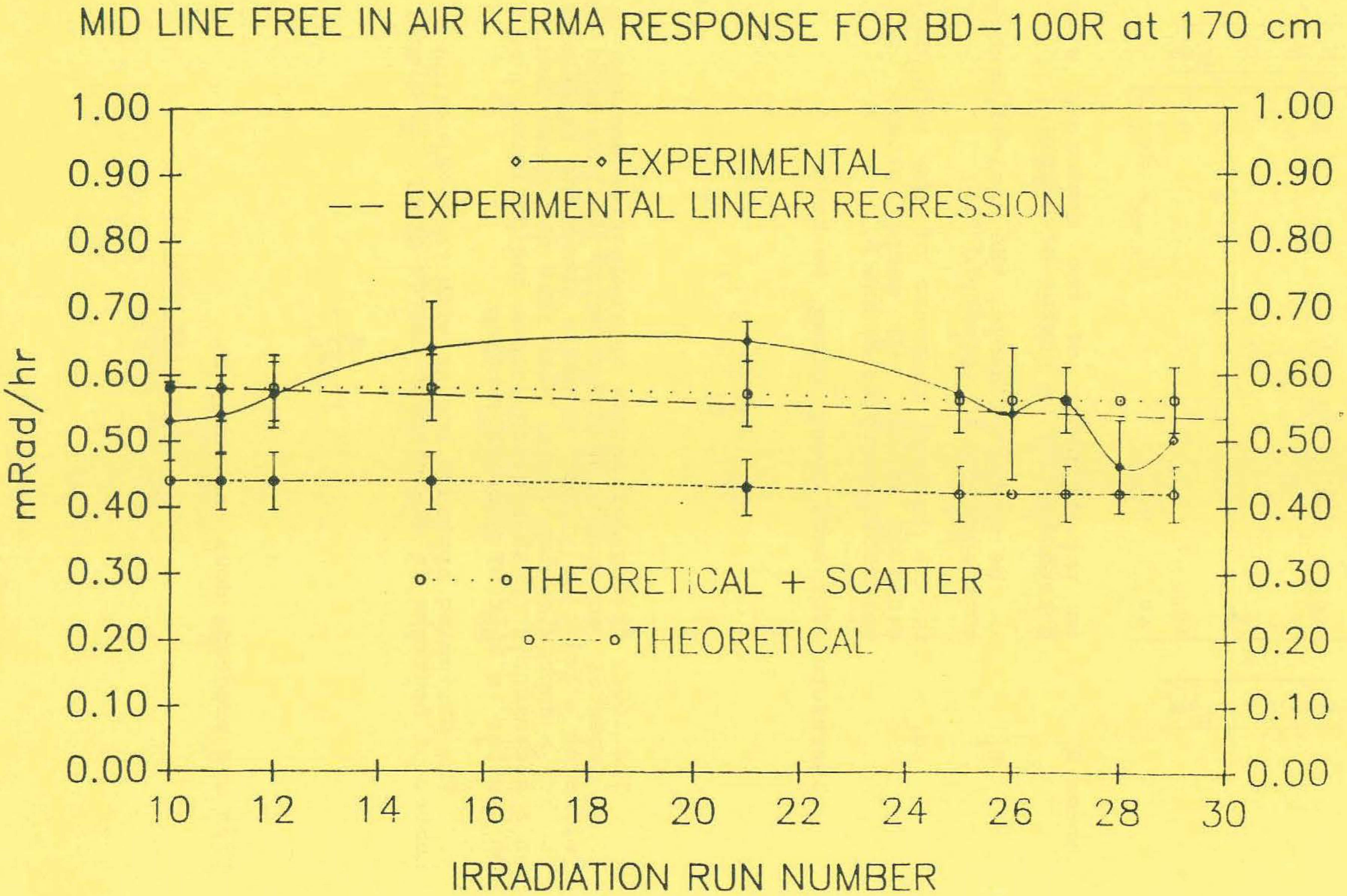


Figure 3 : MLFIAK Theoretical and Measured Kerma Rates

$$
\begin{vmatrix} R_1 \\ R_2 \\ \cdot \\ \cdot \\ \cdot \\ R_{n-1} \\ R_n \end{vmatrix} = \begin{vmatrix} \langle\sigma_{1,1}\rangle & 0 & 0 \cdot \cdot 0 & 0 & 0 \\ \langle\sigma_{2,1}\rangle & \langle\sigma_{2,2}\rangle & 0\ 0 \cdot \cdot & 0 & 0 \\ \cdot & \cdot & \cdot\ 0\ 0 \cdot & \cdot & 0 \\ \cdot & \cdot & \cdot \cdot 0\ 0 & \cdot & \cdot \\ \cdot & \cdot & \cdot \cdot \cdot \cdot & 0 & 0 \\ \langle\sigma_{n-1,1}\rangle & \langle\sigma_{n-1,2}\rangle & \cdot \cdot \cdot \cdot & \langle\sigma_{n-1,n-1}\rangle & 0 \\ \langle\sigma_{n,1}\rangle & \langle\sigma_{n,2}\rangle & \cdot \cdot \cdot \cdot & \langle\sigma_{n,n-1}\rangle & \langle\sigma_{n,n}\rangle \end{vmatrix} \begin{vmatrix} N_1 \\ N_2 \\ \cdot \\ \cdot \\ \cdot \\ N_{n-1} \\ N_n \end{vmatrix} \qquad (1)
$$

where: $R_i$ is the response of the detectors with energy threshold "i", in number of bubbles;

$N_i$ is the neutron fluence, the desired unknown, corresponding to threshold "i";

$<\sigma_{i,j}>$ is the average response of the i-th detector to neutrons in the j-th energy group, i.e. between threshold energies $E_j$ and $E_{j-1}$.

Therefore, for each energy group, we have:

$$
R_i = \sum_{j=1}^{n} \langle\sigma_{i,j}\rangle\ N_j \qquad (2)
$$

The lower triangular matrix approximation assumes that there is no detector response to neutrons below the threshold energy and relies on a relatively flat response above the threshold to make the $<\sigma_{i,j}>$ approximation valid. Note that the nomenclature is that of a microscopic cross section, since the definition of the $<\sigma_{i,j}>$ is similar to that of a cross section.

The stripping approach begins with the evaluation of $N_1$, the number of neutrons in the highest energy group, as simply

$$
N_1 = \frac{R_1}{\langle\sigma_{1,1}\rangle} \qquad (3)
$$

Then one proceeds down in energy to

$$
N_2 = \frac{(R_2 - \langle\sigma_{2,1}\rangle N_1)}{\langle\sigma_{2,2}\rangle} \qquad (4)
$$

and, in general,

$$N_k = \frac{R_k - \{\sum_{j=1}^{k-1} \langle\sigma_{k,j}\rangle N_j\}}{\langle\sigma_{k,k}\rangle} \qquad (5)$$

The values of the $N_i$'s are obtained this way. The method has the advantage of being simple to use, without sophisticated computer analysis required. It does however suffer from error propagation, which can lead to high uncertainties at the lower energies, depending on the statistical accuracy of the data from the higher energy groups.

## PROCEDURE

This research was carried out at the Defence Research Establishment Ottawa (DREO), in Ottawa, Canada. The anthropomorphic phantom was suspended in a harness, as shown in Figure (4), and maintained in a rigorously controlled position with regard to the Cf-252 neutron source. The source was kept in a large shielded container in a separate building, and was brought in position for irradiation by using a rotary crank wire which pushed and pulled it in a stainless steel flexible conduit channelled in a rigid PVC pipe. Positioning of the source was carefully monitored to ensure consistency of the results. The source holder was fixed at 95.5 cm off the floor, exactly at the same level as the detectors installed at the gut location on the phantom. The middle of the phantom was at 170 cm from the source. The detector positions on and in the phantom were the chest, the back gut, the middle gut, the front gut, the right wrist, and the left wrist. The phantom was oriented facing, right hand side to, and back to the source for dosimetry, and facing the source only for spectrometry.

## RESULTS

### (i) Free Field Results

#### a) Dosimetry:

With the calibrated Cf-252 neutron source described before, the kerma rate measured at 170 cm varied from 0.65 to 0.53 mrad/hr (12). Free-field kerma measurements with the BD-100R bubble detectors involved experiments both with and without a shadow bar. The dosimetry results are in excellent agreement with theory.

Figure 4 : Anthropomorphic Phantom Suspension

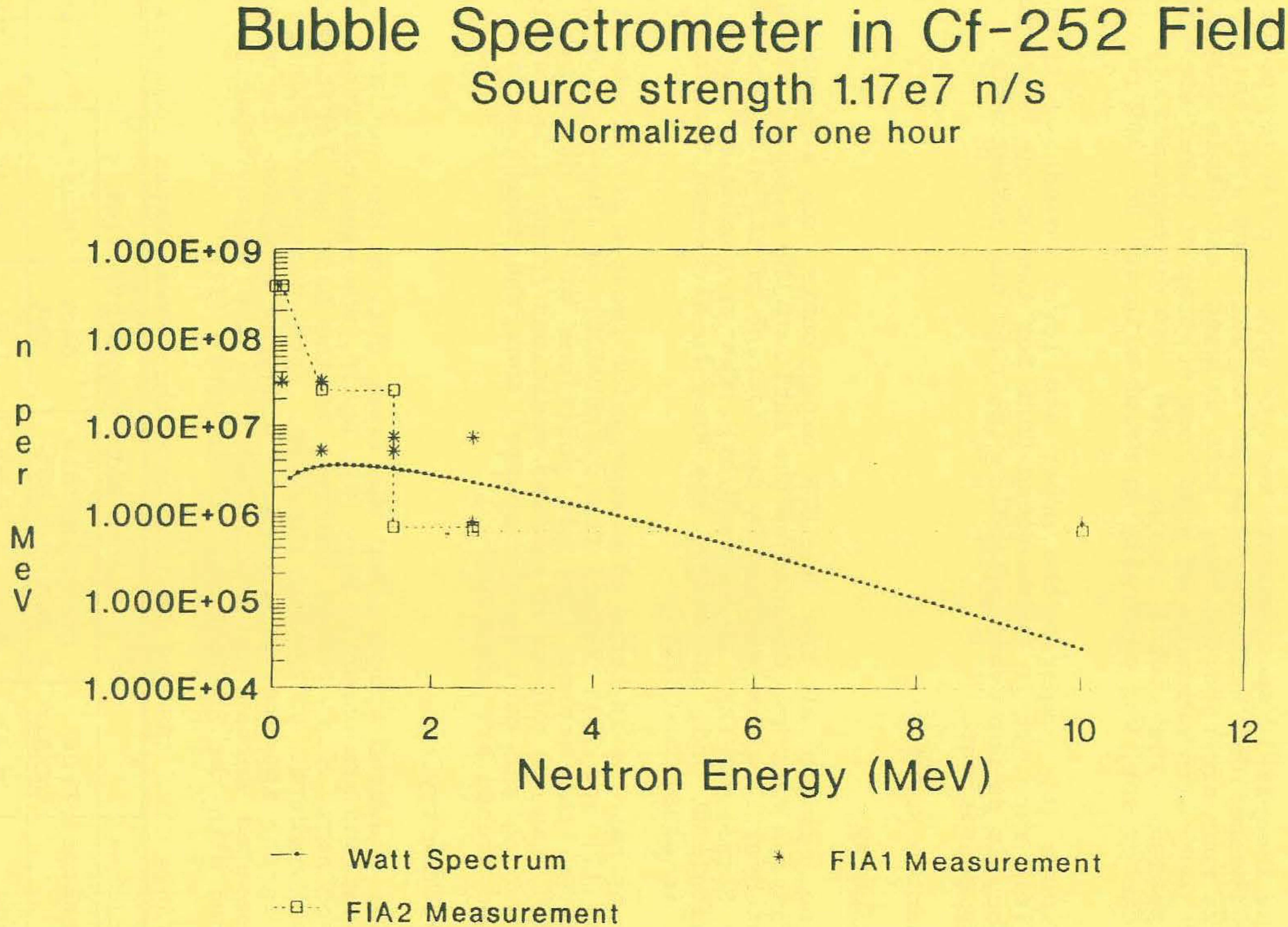


Figure 5 : Bubble Detector Spectrometer Free-in-Air Kerma

b) Spectrometry:

The free-field spectrometry results appear in Fig (5) compared to the theoretical Watt spectrum for Cf-252. The results of two separate runs are reported here, both showing reasonable agreement above 1 MeV, with evidence of some room scatter at lower energies, as expected. The total kerma rate, as determined by the spectrometer set, was generally agreeing with the DB-100R results. (12).

Figure (6) compares the upper and lower bounds of the two free-field runs. It is to be noted that for two of the detectors, these bounds do not overlap, indicating that the detectors are not totally consistent.

ii) Phantom Results

a) Dosimetry

The results of the BD-100R experiments are expressed as transmission factors, defined as the ratio of the measured kerma at the detector location divided by the average of the Mid-Line Free-in-Air Kerma (MLFIAK) (0.58 mrad/hr). The transmission factor is dimensionless, and, obviously, the Free-in-Air kerma transmission factor is equal to unity.

The results in terms of transmission factors are presented in Figures (7) and (8), versus the orientation of the phantom with respect to the source, for all positions of the detectors. As expected, the dosimeters in similar positions (right wrist and left wrist facing and back to the source) show the same results. The expected trends are observed.

b) Spectrometry

The measured spectra for the front gut, middle gut and back gut locations are shown in Fig. (9). Again, the expected trends are observed here, i.e. fewest neutrons at the back gut location and general spectral softening. However, some negative fluences do occur in the spectra, indicated by diagonal lines on the graphs. The measured kermas as determined from the energy spectra are compared with the BD-100R results in Table (II).

Table II. BDS and BD-100R Detectors Kerma Rates Comparison.

| Location→ | Kerma Rate (mrad/hr) ±10% | | | | | |
|---|---|---|---|---|---|---|
| ↓ Detector | Free in Air | Front Gut | Middle Gut | Back Gut | Wrists | Chest |
| BDS | 0.65 | 0.79 | 0.19 | 0.06 | 0.45 | 0.74 |
| BD-100R | 0.58 | 0.82 | 0.22 | 0.05 | 0.49 | 0.71 |
| Difference | 12% | 4% | 16% | 20% | 9% | 4% |

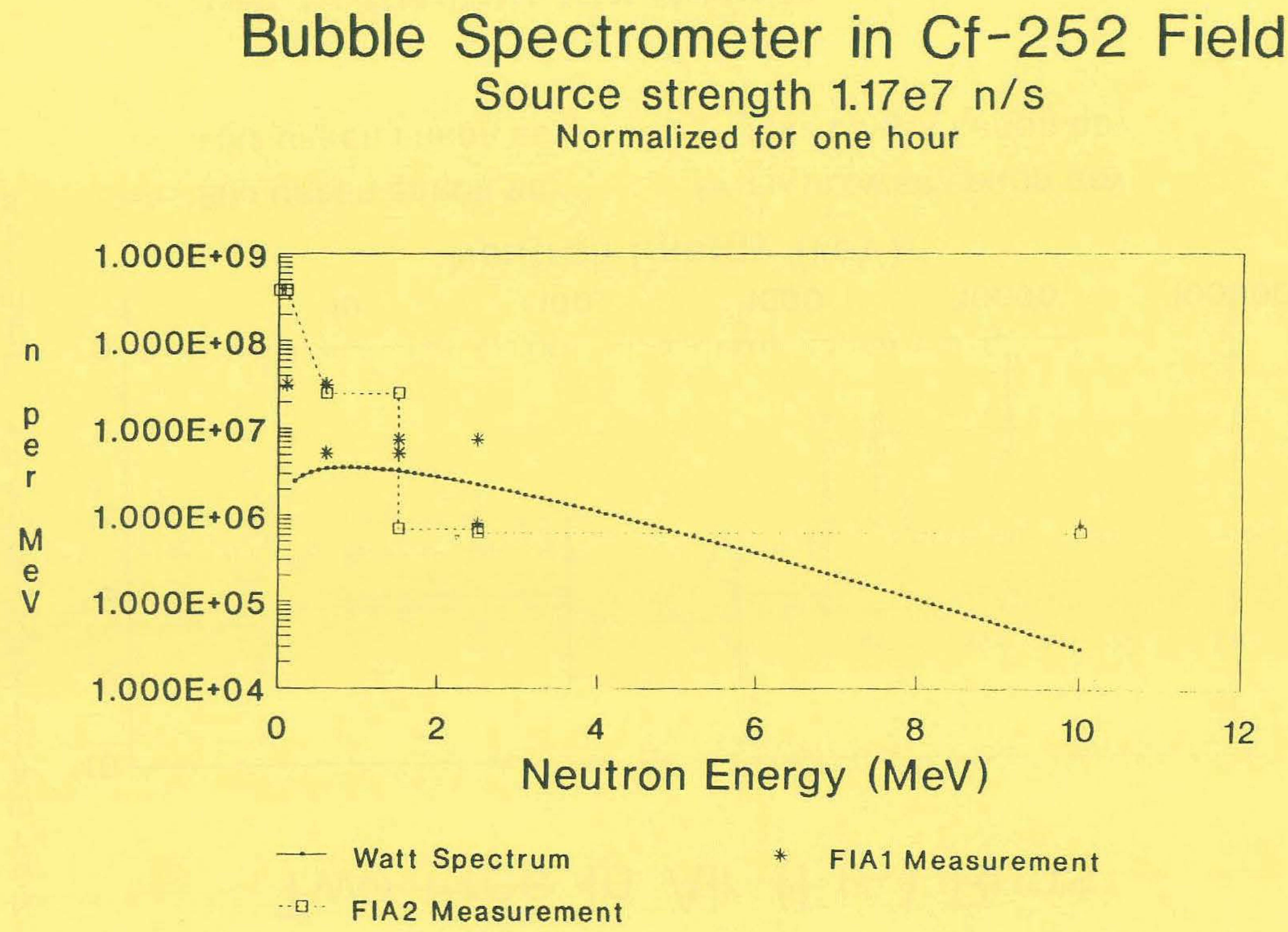


**Figure 5 : Bubble Detector Spectrometer Free-in-Air Kerma**

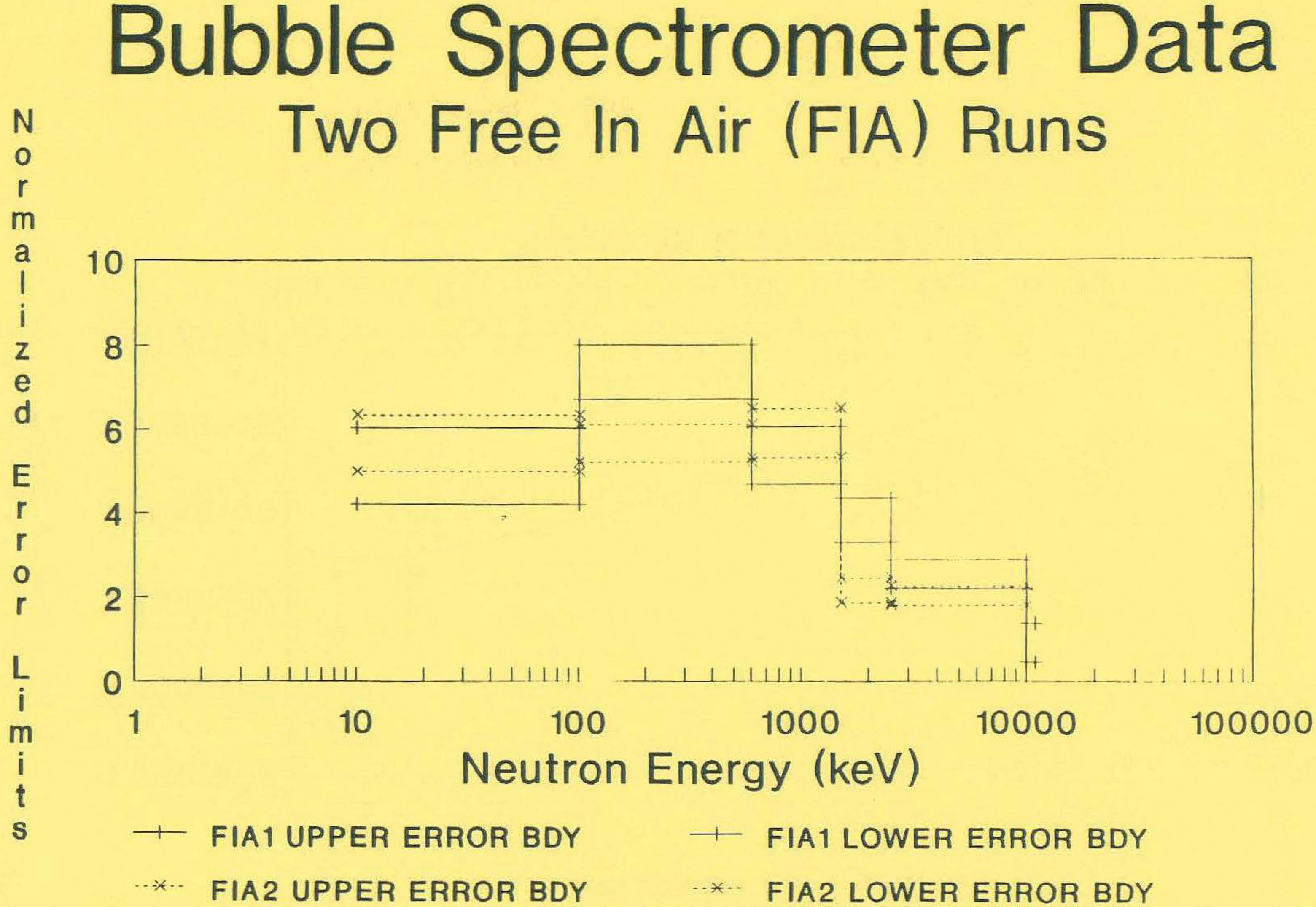


Figure 6 : Free-in-Air Error Boundaries

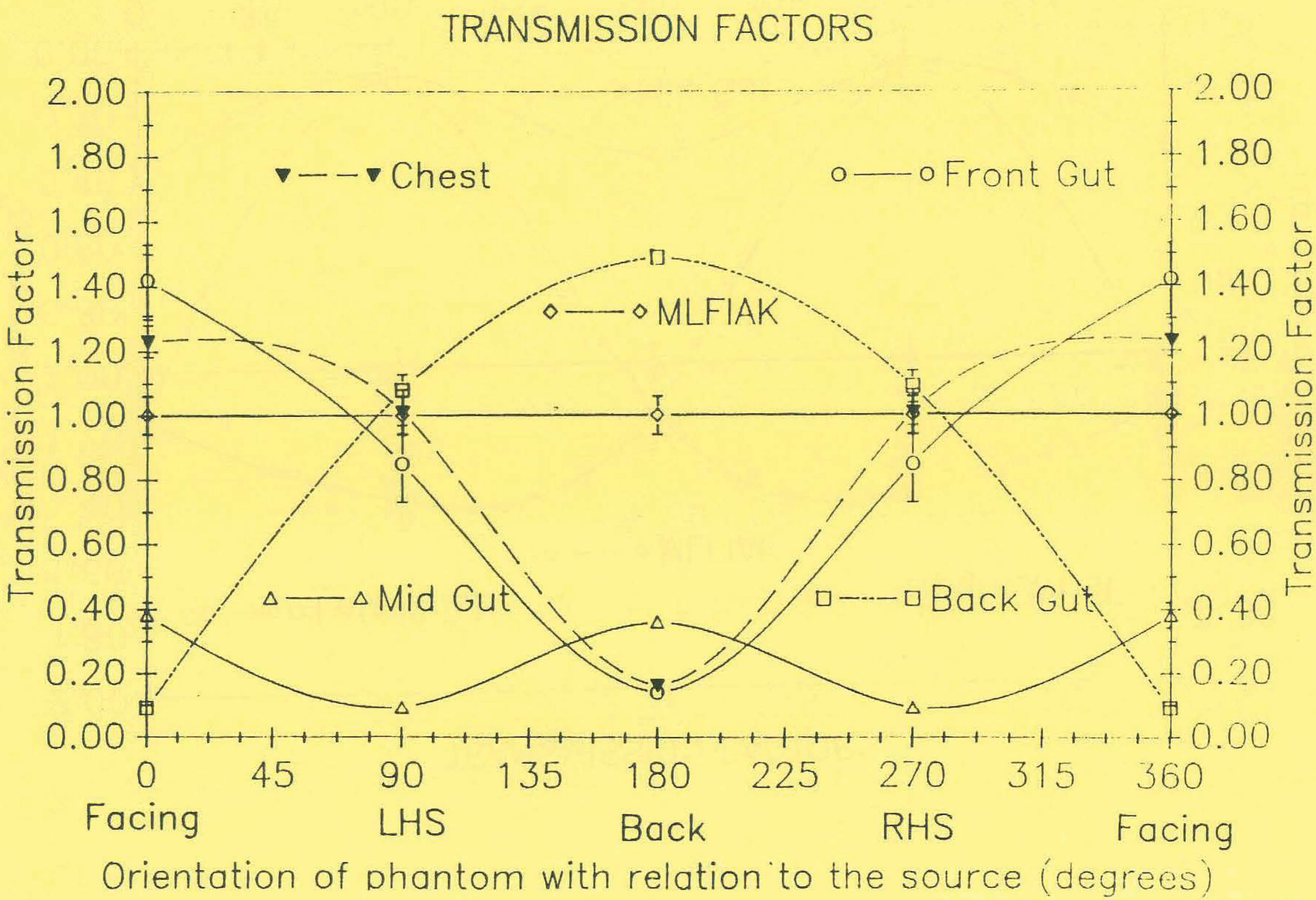


**Figure 7 : Transmission Factors**

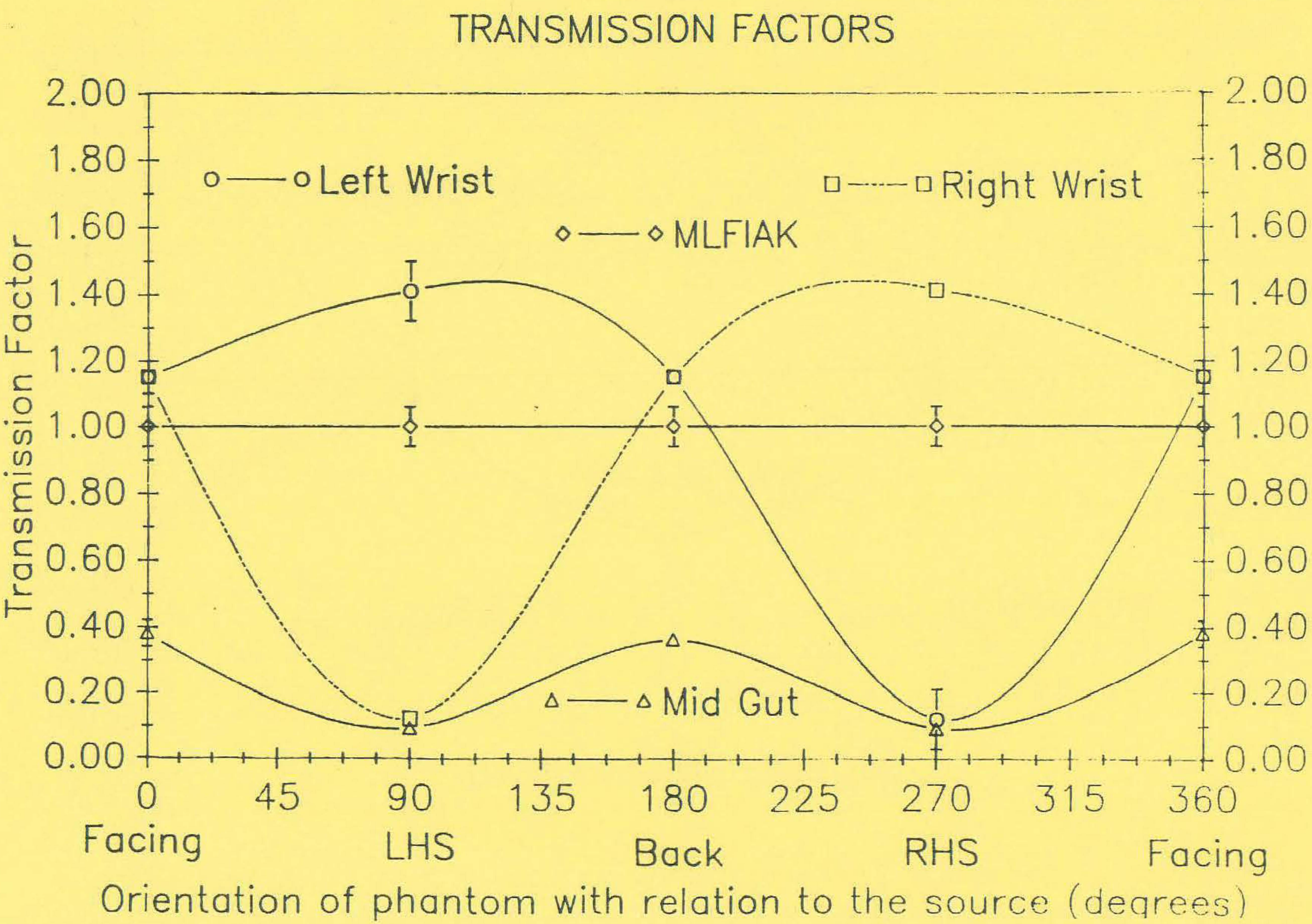


**Figure 8 : Transmission Factors for Wrists**

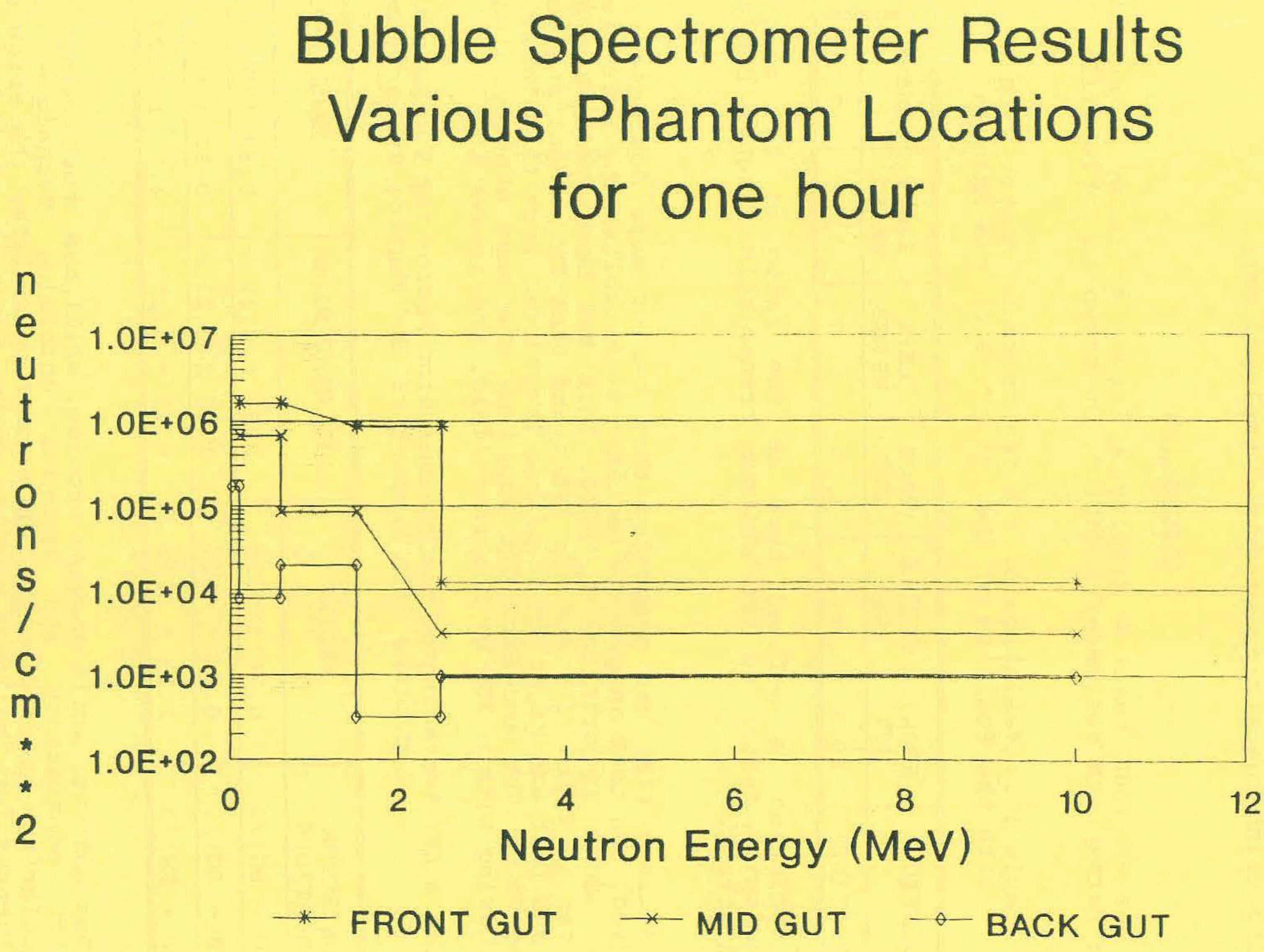


Figure 9 : BDS Results for Gut Locations

The results are in good agreement, permitting the conclusion that the BDS spectrometer set may be used to give crude spectral results using the stripping method employed here.

## DISCUSSION

The BD-100R results display a large variation in measured kerma rates with dosimeter location, as shown in Table (III).

Table III: Variation of the Transmission Factor with with the Position of the Detectors on the Phantom

| LOCATION | FRONT GUT | MIDDLE GUT | BACK GUT | LEFT WRIST | RIGHT WRIST | CHEST |
|---|---|---|---|---|---|---|
| VARIATION* | 10.1 | 4.2 | 16.6 | 11.7 | 11.7 | 7.7 |

* Variation is defined here as the ratio of the maximum transmission factor to the minimum transmission factor for all orientations.

Allison (13) has suggested that two or more dosimeters be employed, and that an average be taken to establish the free-field value, which is critical to NATO. This has been done here and reported in Table (IV) for the Front and Back Gut, Chest and Back Gut, and Left and Right Wrist paired locations. From this Table, a paired Front Gut and Back Gut would be the best choice, always registering within 20% of the free-field, and always low.

Table IV: Averaging of the Transmission Factor for Two Detector Locations with Respect to the Phantom Orientation.

| DETECTOR LOCATIONS | FACING | LEFT HAND SIDE | BACK |
|---|---|---|---|
| (FG + BG)/2 | 0.76 ± 0.15 | 0.97 ± 0.19 | 0.82 ± 0.16 |
| (CH + BG)/2 | 0.66 ± 0.13 | 1.05 ± 0.21 | 0.83 ± 0.17 |
| (LW + RW)/2 | 1.15 ± 0.23 | 0.77 ± 0.15 | 1.15 ± 0.23 |

The BDS set, while showing promise, still has shortcomings in detector consistency and spectral unfolding technique. In particular the spectral unfolding method accumulates the error as the fluences for the lower neutron groups are calculated from the results obtained for the faster groups. This is summarized in Equation (2), and, as more and more terms are added to the summation, the errors progagate greatly. Consequently, the neutron fluences obtained for the slow neutron groups carry relative error often larger than 100%, resulting in some cases in negative fluences determined by this process, and making the information from these BDS detectors of limited value.

The total kerma rate obtained with the BDS set compared well with the kerma rate measured with the BD-100R detectors. In spite of this, the confidence in the spectral results from the BDS detectors is too low to provide sound information. The most important source of error is the spectrum unfolding technique which is such that the results for the low energy neutron groups have an unacceptably high error due to error accumulation. This can be remedied in two ways. The calibration of the detectors by the manufacturer should be carried out more rigorously to provide the $\sigma_{ij}$ coefficients with a much improved accuracy. Second, the error on the response of the detectors ($R_i$) should be kept as small as possible by increasing statistics. For spectrometry reasons, bubble counts of the order of 100-150 bubbles provide a 8-10% statistical error which is too large for accurate spectrum unfolding process. Bubble counts of the order of a thousand or more are necessary for a 3% statistical error or better.

Research and development in this area are carried out strongly and solutions to these problems are being proposed. The temperature dependence is being investigated and studies are on-going on materials that would make the bubble dosimeters temperature independent. The problem of low bubbles counts is also being addressed and a proposed technique based on acoustic waves could permit much larger counts for increased accuracy.

## Conclusions and Recommendations

Neutron transport in air and energy deposition on and in an anthropomorphic phantom, from irradiation with a Californium-252 neutron source, were investigated using superheated drop bubble detectors as dosimeters and spectrometers.

The results showed that the BD-100R reusable bubble detectors were reliable and accurate, and that they could be indeed recommended as personal dosimeters provided the temperature effects are accounted for. The contribution of the scattered neutrons could be measured accurately and was not negligible. The average Free-in-Air Kerma was measured within 3% of the theoretical value.

The measured kerma in the phantom was found to be dependent on the orientation of the phantom and location of the dosimeters on the body. Neutron attenuation in the body was measured as a factor of 10. Considering that the neutron risk assessment appears underrated, a ten-fold variation in the measured kerma is not acceptable.

This experiment allows the recommendation that a minimum of two dosimeters should be worn close to several vital and radiosensitive parts of the body, the preferred locations determined as the front gut and the back gut. Additional detectors, such at the wrist locations, may be useful depending on the nature of the work involved.

This work was a first attempt at using the bubble spectrometer set for dosimetry purposes on an anthropomorphic phantom. Limited sound data were obtained, with the total kerma measured being within 11% fo the value obtained with the BD-100R detectors. Furthermore, an error evaluation showed how error accumulated through the spectrum unfolding process to an unacceptable value.


## ACKNOWLEDGEMENTS

This work was made possible by the Master's Degree program of the Canadian Armed Forces, and by the collaboration of the personnel of the Defence Research Establishment Ottawa, to which the authors express their appreciation, in particular to Dr. F Szabo, Head of the Radiation Effects Section of DREO, and to Mr. J. Brisson, of the Radiation Effects Section of DREO. Thanks are also due to Royal Military College, for the financing of the detectors, and to Dr. R.F. Mann, former Head of the Department of Chemistry and Chemical Engineering.


## REFERENCES


1. Commission of European Communities: Fourth Symposium on Neutron Dosimetry; Munich-Neuherberg (1981).

2. T. Cousins and L.P. Rushton, "Anthropomorphic Phantom Radiation Dosimetry at the NATO Standard Reference Point at Aberdeen Proving Ground"; Defence Research Establishment Ottawa Report No. 968, April 1987.

3. T. Cousins and D.C. Kaul, "Anthropomorphic Phantom Radiation Dosimetry at 400 m from a Fission Source", Trans. Am. Nucl. Soc. 57, p.218 (1988).

4. International Commission on Radiation Units and Measurements; "Neutron Dosimetry for Biology and Medicine"; Report No. 25, ICRU Publications, Washington, D.C. USA (1976).

5. Ing H. and Birnboim H.C.; "A Bubble Damage Polymer Detector for Neutrons"; Nuclear Tracks and Radiation, 8, p. 285 (1984).

6. Ing H.; "Bubble Damage Polymer Detectors for Neutron Dosimetry"; Fifth Symposium on Neutron Dosimetry, Neuherberg, Germany (1984).

7. H. Ing, "A Neutron Detector Based on Nucleation of Superheated Liquids"; Proc. 1985 Workshop of the Research Study Group on the Assessment of Ionizing Radiation Injury in Nuclear Warfare, Ottawa, Ont., Canada (1985).

8. T. Cousins, K. Tremblay and H. Ing, "The Application of the Bubble Spectrometer to the Measurement of Intense Neutron Fluences and Energy Spectra"; IEEE Trans. Nucl. Sci., 37, 6, p.1769 (1990).

9. Stoddard D.H. and Hootman H.E.; "$^{252}Cf$ Shielding Guide"; E.I. Dupont de Nemours & Co.; Savannah River Laboratory, Report DP-1246 (1971).

10. Bleek N.M., Glastein E. and Haybittle J.L., Ed.; "Radiation Therapy Planning"; Marcel Dekker Inc., New York, N.Y., USA (1983).

11. Attix F. and Roesch W., Ed.; "Radiation Dosimetry" (2nd Ed., Vol.1); Academic Press, New York, N.Y., USA (1966).

12. Desnoyers G.J.R.; "Neutron Dosimetry Using Bubble Detectors and an Anthropomorphic Phantom"; Master's Degree Thesis, Royal Military College of Canada, Kingston, Ontario, Canada (1990).

13. Allison J.W.; "Status of Military Dosimetry and Some Options for the Future"; Department of Defence Support Materials Research Laboratories, Melbourne, Australia, 4QWG/NBCD Meeting (1982).